Mon. Not. R. Astron. Soc. **370,** 1783–1789 (2006) doi:10.1111/j.1365-2966.2006.10588.x

Wide-field Adaptive Optics correction using a single rotating laser guide star

T. J. Morris★ and R. M. Myers

Centre for Advanced Instrumentation, Department of Physics, University of Durham, South Road, Durham DH1 3LE

Accepted 2006 May 18. Received 2006 May 15; in original form 2006 February 1

ABSTRACT

The problem of providing Adaptive Optics (AO) correction over a wide field of view is one that can be alleviated by using multiple conjugate AO (MCAO), or a low-altitude Laser Guide Star (LGS) that is projected to an altitude below any high layer turbulence. A low-altitude LGS can only sense wavefront distortions induced by low-altitude turbulence, which is dominated by a strong boundary layer at the ground. Sensing only the wavefront from this layer provides an AO system with a more spatially invariant performance over the telescope field of view at the expense of overall correction. An alternative method for measuring a ground-layer biased wavefront using a single rotating LGS is presented together with a numerical analysis of the wide-field performance of an AO system utilizing such a LGS. System performance in *H* and *K* bands is predicted in terms of system Strehl ratio, which shows that uniform correction can be obtained over fields of view of 200 arcsec in diameter. The simulations also show that the on-axis performance of a LGS utilizing Rayleigh backscattered light will be improved.

Key words: instrumentation: adaptive optics.

1 INTRODUCTION

Single Laser Guide Star (LGS) Adaptive Optics (AO) systems, first introduced by Foy & Labyrie (1985), currently have a restricted field of view brought about by the effect of angular anisoplanatism. Tomographic multiple conjugate AO (MCAO) can provide diffraction-limited performance over a wider field of view (Beckers 1989). Examples of planned MCAO systems can be found for the *Gemini* South Telescope (Ellerbroek et al. 2003), for the Large Binocular Telescope (Gässler et al. 2004) and for the Very Large Telescope (Hubin et al. 2002). A simpler form of tomographic AO, which corrects only image distortions that are induced only by atmospheric turbulence at altitudes near to the ground, has been proposed (Sharples, Myers & Walton 2000; Rigaut 2002). This increases the angular diameter of the corrected field at the expense of overall performance. Such so-called ground-layer AO (GLAO) methods can provide a partially corrected wavefront over fields of view measuring arcminutes in diameter by correcting for atmospheric turbulence that is common to all field angles. As the overall degree of correction is still affected by higher layer unsensed or uncorrected turbulence, GLAO is sometimes referred to as a seeing-improvement technique.

The principle behind GLAO is the determination of turbulence at, or near, the telescope pupil. Two methods are currently being developed that will determine a ground-layer-induced wavefront distortion: (i) Wavefronts from several reference sources distributed within the telescope field of view can be analysed for common wavefront terms (Ragazzoni, Marchetti & Valente 2000), (ii) A low-altitude Rayleigh LGS that cannot sense high-altitude turbulence is projected preferably to an altitude just below the higher turbulent layers [see Tokovinin et al. (2004) for example].

A third method, which is analysed in this paper, samples several paths through the atmosphere and optically co-adds the wavefront from each sampled path within the time taken for a single wavefront sensor (WFS) exposure. A simple means for creating a system that achieves this using a single LGS is also presented. Results of numerical simulations of the technique are discussed and compared to the performance of AO systems using a single LGS over a range of altitudes from 8 km, corresponding to the altitude of a LGS utilizing Rayleigh backscattered photons, to 90 km, corresponding to the altitude of a LGS that uses sodium resonance backscattering. Finally, the performance of an AO system with a rotating LGS operating in the near-infrared (NIR) is modelled.

2 DESCRIPTION OF THE TECHNIQUE

A simple method of sampling several distinct paths through the atmosphere using a single LGS is to rotate the LGS on the sky at a fixed angular distance from a defined field point. The LGS can then trace a circular path on the sky around this point, and will sample the wavefront from several distinct paths through the atmosphere. This LGS motion is then corrected using a fast-steering optic, providing an angular offset to the returning LGS light that is in phase with the launch offset. In this manner, the circular motion of the LGS on the

★E-mail: t.j.morris@durham.ac.uk (TJM)

sky will be removed, and a stable wavefront reference source will be created. It should also be noted that the technique presented in this paper emulates the optimum guide-star geometry for GLAO as determined by Tokovinin (2004).

If the angular frequency of rotation is equal to the frame rate of the WFS, many different paths through the atmosphere will be sampled within a single WFS frame. The number of independent paths depends upon the pulse rate (if pulsed) of the laser. A pulsed output laser is assumed in the following discussion, but the technique is equally applicable to continuous wave (CW) lasers. Distortions that are due to atmospheric turbulence that are common to all LGS paths, i.e. low-altitude turbulence, will be co-added within the single WFS frame. For turbulent layers not situated at the telescope pupil, the wavefront sampled by the rotating LGS will change with each output pulse from the laser. Once each individual wavefront has been optically co-added, the wavefront distortions observed in the LGS wavefront due to high-layer turbulence will blur. The magnitude of this blur is defined by the overlap between the circular areas illuminated by light from the LGS at the altitude of the turbulent layer. Once this overlap has increased to the point where the wavefronts show minimal correlation (either by increasing the angular diameter of LGS rotation or because of the presence of higher altitude turbulent layers) the effect of the corresponding wavefront distortions will be reduced in the rotating LGS wavefront. This will bias the measured wavefront towards sensing low-altitude turbulence.

As shown by Wilson & Jenkins (1996), decorrelation of high radial order Zernike modes (Noll 1976) with increasing pupil offset occurs at a faster rate than for lower radial order modes. This property means that the rotating LGS will be able to sense low-order wavefront terms from turbulent layers that are within some small vertical distance of the telescope pupil. This implies that low-order AO correction using a rotating LGS will not only correct the ground-layer, but also correct turbulent layers near the ground. Low-order modes introduced into the rotating LGS wavefront by turbulent layers up to some non-zero altitude will be common to field angles equal to that of the angular radius of LGS rotation. The maximum wavefront correlation altitude depends upon the angular diameter of LGS rotation.

2.1 Experimental implementation

The concept of optically co-adding light from several wavefront reference sources on a single WFS image to improve signal-to-noise ratio (SNR) is one that was introduced by Ragazzoni (1999). However, this technique is best implemented using a pyramid WFS (Ragazzoni & Farinato 1999), whereas the technique presented here is equally applicable to almost any type of WFS. Optically co-adding light from several guide stars using a non-pyramid WFS without the rotation of a LGS, although possible, would require complex image plane slicing and recombination techniques. One possible LGS implementation using a diffractive optic conjugated to the telescope pupil-plane is discussed later.

If a LGS is rotated, an open-loop correction system must be employed to correct for the observed rotation of the LGS on the sky. The LGS rotation is equal to the frame rate of the LGS WFS, and therefore cannot be corrected using a closed-loop system. To achieve open-loop correction, a synchroniztion signal from the LGS offset mechanism in the laser launch system must be passed to a LGS offset corrector before the LGS WFS. The amplitude and phase of the correction applied to the rotating LGS could then be adjusted until the apparent diameter of the LGS reached a minimum value, thus ensuring effective cancellation of the LGS rotation.

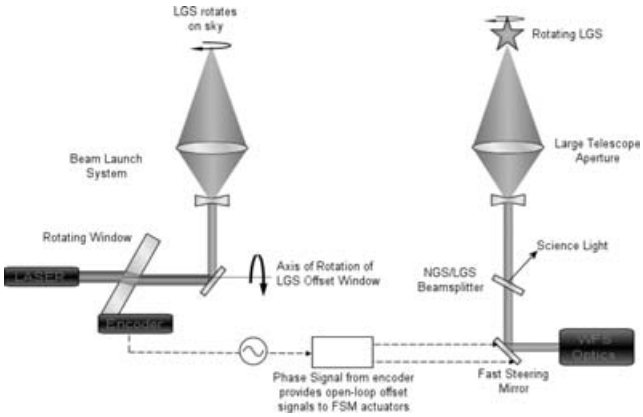

Figure 1. Diagram showing method for creating a rotating LGS using a tilted rotating window in the laser launch path and a FSM providing correction of the observed rotation.

Creating a rotating LGS requires very few modifications to an AO system that already employs a LGS as a wavefront reference. One possible implementation is shown in Fig. 1, where a fast-steering mirror (FSM) corrects for the offset induced in the laser launch system by a rotating tilted glass plate. The glass plate rotates once per WFS frame, and an optical encoder provides a synchroniztion signal to a FSM placed before the LGS WFS. A sinusoidally varying offset voltage is applied to each FSM actuator to induce a counter-rotation in the LGS WFS field angle. This technique assumes that rotating the glass plate at the WFS frame rate of up to 1 kHz (corresponding to 60 000 rpm) is a feasible option. This approach becomes less technically challenging for WFSs running at slower frame rates.

Several alternative methods exist for creating an open-loop offset and correction system that does not rely on ultrafast rotating glass plates. The angular frequency of rotation can be slowed if a precision-machined optic or transparent phase plate, as described in Kolb et al. (2004), is used in place of the rotating glass window. A repeating pattern can be created in an annulus around the edge of the optical element that will rotate the LGS on the sky as is shown in Fig. 2. This allows the angular frequency of rotation of the window to be reduced by a factor equal to the number of times the offset pattern is repeated.

Rather than rotating optics, FSMs could be used exclusively to create and correct for the LGS offset. FSMs with resonant frequencies near the kHz range are commercially available that can correct for a 120 arcsec off-axis angle on an 8-m telescope. Acousto-optic devices also exist that could provide this offset at high rotational frequencies.

An alternative approach to the problem is to use two non-rotating Diffractive Optical Elements (DOEs). The first is positioned inside the launch telescope and creates several static, offset LGS. This approach to creating multiple guide stars was taken by Lloyd-Hart et al. (2005) to create a five-star asterism. A second DOE is placed in front of the LGS WFS in a plane conjugate to the telescope pupil that recombines the light from each individual LGS. To the knowledge of the authors, beam recombination of Rayleigh backscattered light has not been attempted using a DOE. However, the combination of multiple laser beams using a DOE has been demonstrated (Tondusson et al. 2001) with 82 per cent of the light from four diffraction-limited beams being combined into a single diffraction-limited beam. The dual DOE method is inherently less light efficient than the other methods presented, as a relatively large fraction of light is lost (compared to reflection from a suitably coated mirror or

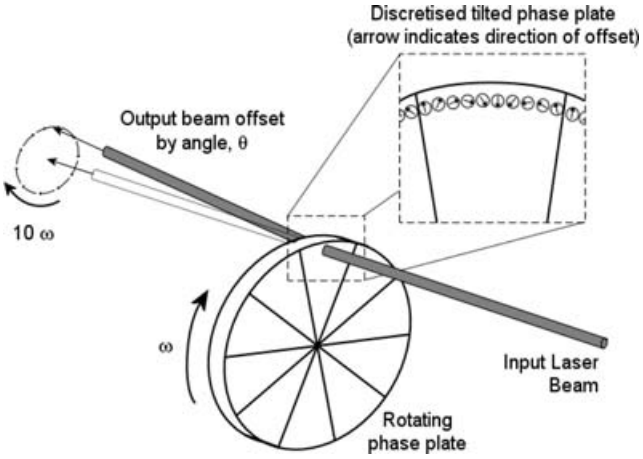

Figure 2. Diagram showing method for creating a rotating LGS using a rotating optic in the laser launch path that contains a repeating pattern that can offset the output laser beam. A pattern of 10 wavefront tilts (shown as circular spots in the diagram) is repeated on each of the 10 segments shown on the rotating phase plate. The slope of the wavefront introduced by each circular spot is rotated by $11\pi/50$ radians with respect to its neighbouring spot to account for both the rotation of the LGS by 2π within the 10 spots comprising a single segment and the rotation of the phase plate. The rotational frequency of the LGS will therefore be 10 times that of the rotating phase plate. The rotational frequency of the tilted spots is synchronized to the pulse rate of the laser.

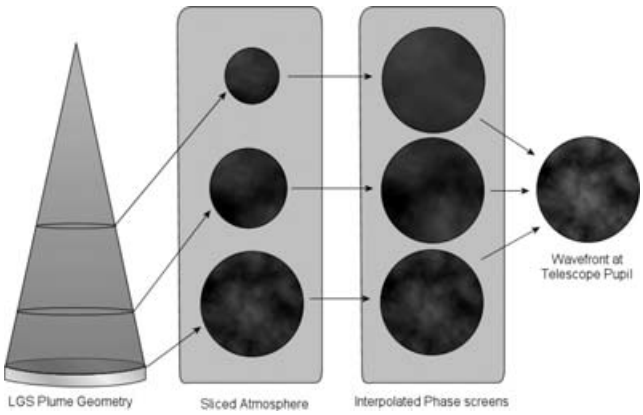

Figure 3. Diagram showing method for creating LGS wavefronts from a vertically distributed turbulence profile. Wavefronts are sliced based upon the geometric cone of atmosphere illuminated by a LGS at a finite distance being observed by a telescope with an annular aperture. The phase screen from each turbulent layer then undergoes pixel interpolation to match the number of pixels defined across the telescope aperture. The sliced and interpolated phase screens are then summed to determine the LGS wavefront at the telescope pupil.

antireflection coated offset plate) when diffractive optics are used; however this approach does not require open-loop correction of the LGS rotation, substantially reducing overall system complexity. The performance of a double DOE LGS will be identical to that of a rotating LGS, assuming that the number of independent LGS paths traced through the atmosphere and LGS offset angles is equal. The results of the numerical model describing the performance of a rotating LGS are therefore equally applicable to a double DOE LGS.

2.2 Description of the numerical model

A numerical model was designed to study the performance of a rotating LGS under realistic atmospheric conditions. To simulate the rotating LGS, a set of field positions was defined based on the angular diameter of the LGS rotation. For a Rayleigh laser, 10 pulses per frame were defined, making the angular rotation between each pulse around the circular path of the rotating LGS 0.2π. A sodium LGS does not require a pulsed output, but for comparative purposes and computational simplicity, a pulsed sodium laser was assumed that also provided 10 laser pulses per WFS frame.

For each LGS field point that had been defined, the volume of atmosphere illuminated by the backscattered light from the finite altitude LGS was determined. At each layer, the two-dimensional section of the turbulent layer sampled by the LGS was sliced and a set of turbulent paths through the atmosphere defined. Phase screens sliced from higher turbulent layers were rescaled via pixel interpolation to the diameter (in pixels) of the telescope pupil. This allowed the turbulent layers sampled from a single LGS field point to be co-added to form a single-phase screen positioned at the telescope pupil. This method is illustrated in Fig. 3. The wavefronts observed by each LGS were then added and scaled by the number of laser pulses to create the rotating LGS signal. Science paths were defined as a path through the atmosphere that originated from a point source positioned at infinity at an off-axis angle relative to the centre of LGS rotation. Science paths describing field angles from 0 arcsec (on-axis) to 180 arcsec off-axis were simulated using the same method used to simulate the LGS path except that the diameter of the science beam at each turbulent layer remained constant. Therefore no rescaling of the science path phase screens was required.

Global tip/tilt and piston were removed from both the LGS and science paths as would effectively be the case in an on-sky system. The rotating LGS signal was then subtracted from each science wavefront and the residual wavefront variance determined at points across the 180-arcsec field of view under investigation. To obtain a statistically relevant sample, the process was repeated for a thousand random von Kármán (von Kármán 1948) atmospheres, each with an identical vertical distribution and characteristic turbulent scale.

Throughout this paper, all stated angular diameters of LGS rotation are defined relative to the on-axis field angle of a telescope and denoted by the symbol α. All off-axis science paths are described by the parameter β, where β is the angle in arcseconds of the off-axis field point from the centre of rotation of the LGS. It should be noted that all wavefront variances are calculated at a wavelength of 500 nm. Converting a wavefront variance in terms of Strehl ratio at this wavelength is outside the limits of the Maréchal approximation. The Maréchal approximation (Maréchal 1947) was used to determine system performance in terms of Strehl ratio at NIR wavelengths. *H* and *K* wavelength bands were defined as monochromatic at their central wavelengths of 1.65 and 2.2 μm, respectively.

3 RESULTS

A five-layer von Kármán atmosphere was modelled above a telescope with an 8-m primary aperture and 1-m secondary obscuration. An outer scale of 30 m was assumed and an r_0 of 0.14 m was used. A five-layer atmosphere was used to achieve high resolution in the vertical distribution of turbulent layers in the first kilometre above the telescope pupil. Table 1 describes the three distributions that were defined to correspond to different GLAO conditions. They are summarized as follows:

(i) 'good' GLAO conditions; the majority of the turbulence is contained within the ground layer,

Table 1. Turbulent profiles used in model corresponding to *good*-, *median*- and *bad*-seeing conditions.

Altitude	0.0	0.5	1.0	2.5	10.0
Good	0.5	0.05	0.05	0.2	0.2
Median	0.3	0.1	0.2	0.2	0.2
Bad	0.2	0.1	0.1	0.3	0.3

Altitudes are in km. The numbers for the *good*, *median* and *bad* profiles correspond to the relative turbulent strength of the layer at that altitude.

(ii) 'median' GLAO conditions; the majority of the turbulence is contained within the first kilometre and

(iii) 'poor' GLAO conditions; turbulence at mid- and high-altitude layers dominates the turbulent profile.

The performance of a rotating LGS modelled at a distance of 90 km from the telescope primary mirror was compared to the performance of a static LGS created at an identical altitude. The angular diameter of the circular path followed by the rotating LGS was initially set to 60 arcsec. The *median* atmospheric profile was used.

As shown in Fig. 4, the on-axis residual wavefront variance of the science path, after the LGS wavefront has been subtracted, increased as the angular diameter of rotation increased from 0 to 60 arcsec. However, the residual wavefront variance at field angles greater than 25 arcsec was improved by the rotation of the LGS. The wavefront variance at field angles between 0 and 40 arcsec showed very little variation, implying a uniform degree of correction across a field of this angular extent under median turbulent conditions. A decrease in residual wavefront variance corresponds to an increase in performance of an AO system utilizing a rotating LGS.

The effect of changing the distance of the LGS from 90 km (approximately that of a sodium LGS) to a distance of 20 km, thereby simulating the effect of LGS rotation on a LGS utilizing Rayleigh backscattering, is shown in Fig. 5. Here, the effect of LGS rotation showed a decrease in residual wavefront variance at all field angles. This effect is due to anticorrelation between turbulent wavefronts at high-altitude layers as sampled by light from the science and LGS paths, and is commonly referred to as focal anisoplanatism (FA).

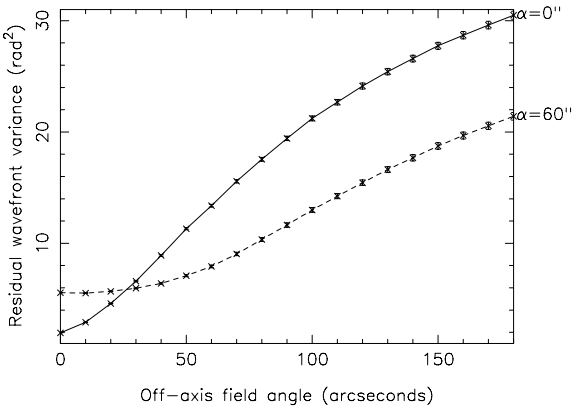

Figure 4. Performance of rotating LGS created at an altitude of 90 km above an 8-m telescope aperture. An angular diameter of LGS rotation (denoted by α) of 60 arcsec has been modelled, as well as the performance of a static LGS ($\alpha = 0$ arcsec) at the same altitude. The residual wavefront variances in science paths at points in the field up to 180 arcsec off-axis after subtraction of the rotating LGS signal are plotted. The median atmospheric profile defined in Table 1 was used. Error bars show 1σ confidence level determined from a bootstrap of 1000 random phase screens.

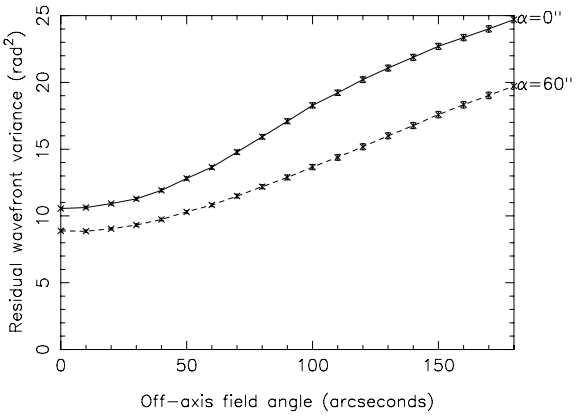

Figure 5. Performance of rotating LGS created at an altitude of 20 km above an 8-m telescope aperture. Angular diameters of rotation (denoted by α) of 60 arcsec have been modelled, as well as the performance of a static LGS ($\alpha = 0$ arcsec) at the same altitude. The residual wavefront variance in science paths at angular offsets in the field up to 180 arcsec off-axis after subtraction of the rotating LGS wavefront is plotted. The median atmospheric profile defined in Table 1 was used. Error bars show 1σ confidence level determined from a bootstrap of 1000 random phase screens.

The cause of FA is the difference in diameter of the illuminated footprint between the LGS and infinity-conjugated science paths at any non-zero altitude turbulent layer. This induces a phase change in the LGS wavefront that is not identical to the phase change induced in the science path wavefront. As the difference in diameter between the two beam footprints increases, so does the wavefront variance between the two associated paths. The variance can increase to the point where removing the phase change in the LGS wavefront can improve the correlation between LGS and science path wavefronts.

This argument is supported by the result that on-axis correction was not improved when a LGS at 90-km distance was rotated by $\alpha = 60$ arcsec. A 90-km LGS exhibits much less error due to FA than a 20-km LGS; therefore the 90-km LGS rotation angle must be smaller to improve on-axis performance. The critical angle at which this occurs has not been investigated here. For LGS AO systems that use multiple 90 km altitude LGSs to improve on-axis correction by reducing FA, the LGS angular separation must be less than 60 arcsec to improve on-axis performance with the atmospheric turbulence profile used here. In this case, a multiple LGSs system would not reduce FA, but create a GLAO system.

The effect of changing the angular diameter of the circular path followed by the rotating LGS is shown in Fig. 6. For a 20-km LGS, the angular diameter of rotation was increased from 0 to 120 arcsec. Optimum on-axis LGS performance was observed with an α of 40 arcsec. The most uniform correction across a 2-arcmin field (i.e. an off-axis angle, β of 60 arcsec) was observed when α was 120 arcsec. Residual wavefront variance at any value of β can be reduced by rotating the LGS on the sky.

The effect of changing the vertical distribution of turbulence while keeping r_0 constant is shown in Fig. 7. Changing the vertical distribution of turbulence will have a large effect on any AO system that utilizes ground-layer correction to provide a wide corrected field of view. Only a slight increase in residual wavefront variance was observed when the vertical distribution of turbulence was changed from the *good* to the *median* profile. This change examined the effect of keeping high-altitude turbulence (defined here as turbulent layers at altitudes greater than 1 km above the telescope pupil)

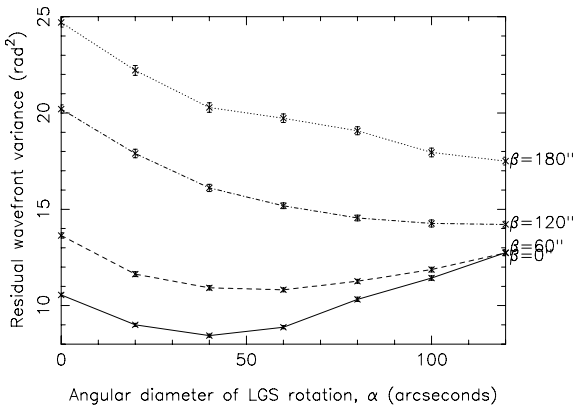

Figure 6. Performance of rotating LGS created at an altitude of 20 km above an 8-m telescope aperture. Angular diameters of rotation between 0 and 120 arcsec have been modelled. The residual wavefront variance in science paths at four angular offsets in the field (denoted by β) up to 180 arcsec off-axis after subtraction of the rotating LGS wavefront is plotted.

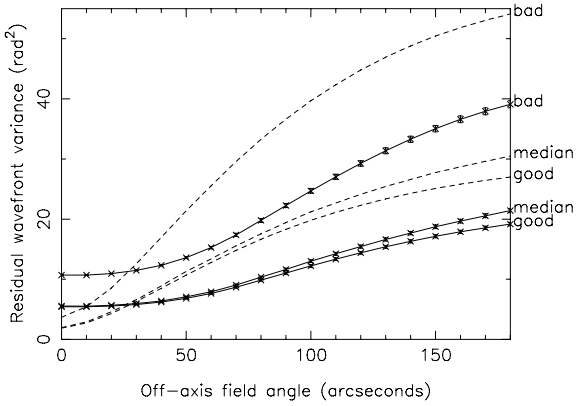

Figure 7. Performance of rotating LGS created at an altitude of 90 km above an 8-m telescope aperture under atmospheric profiles defined in Table 1. Solid lines plot the residual wavefront variance between LGS and science paths when a LGS rotation of $\alpha = 60$ arcsec is set. Dashed lines show performance of a non-rotating LGS under identical atmospheric r_0 and vertical turbulence distribution for comparison.

constant while shifting the concentration of low-altitude turbulence from the ground layer towards layers at 0.5 and 1 km above the telescope pupil. The observed 1.8 per cent change in residual wavefront variance between the *good* and *median* plots shows that a 60 arcsec rotating LGS was relatively insensitive to variations in the distribution of turbulence within the first kilometre on an 8-m telescope. Altering the balance of turbulence such that the majority of turbulence lay outside the first kilometre had a large effect on the residual wavefront variance. This would be observed with any system that determined a ground-layer wavefront only. However, the radius of the field where the residual wavefront variance showed little change remained constant, for example a flat-field of 40 arcsec diameter remained a flat-field of 40 arcsec diameter if the vertical distribution of turbulence changed from the *median* to the *bad* profile, although the overall degree of correction was reduced. This performance demonstrates the suitability of a rotating LGS implementation as a wide-field seeing-improvement system providing partial correction over a wide field defined by the angle of LGS rotation.

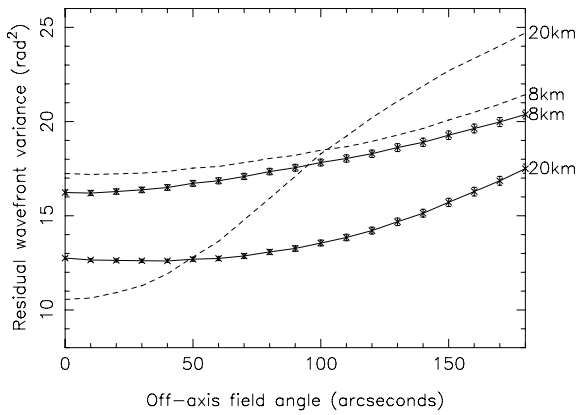

Figure 8. Performance of static (dashed line) and $\alpha = 120$ arcsec (solid line) rotating LGS created at altitudes of 8 and 20 km above an 8-m telescope aperture under the defined median atmospheric profile. Plots were made under identical atmospheric r_0 and vertical turbulence distribution.

A comparison was made between the rotating LGS and a low-altitude LGS. Creating a low-altitude LGS is currently the only alternative method of determining a GLAO wavefront using a single LGS. A comparison between these two techniques is shown in Fig. 8. In this case, the LGS at 8 km did provide a wide flat-field of correction, but still suffered from the problem of anticorrelation of higher layer turbulence contaminating the LGS wavefront. The overall performance was poorer than that of the 20 km rotating LGS ($\alpha = 120$ arcsec) at all field angles out to 180 arcsec. As is shown, once an $\alpha = 120$ arcsec rotation of the 8 km distant LGS was introduced, a decrease in on-axis residual wavefront variance was observed, as was seen with the 20 km distant rotating LGS. A rotation angle of $\alpha = 120$ arcsec degrades on-axis performance for both 8 and 20 km LGSs compared to both a non-rotating and $\alpha = 60$ arcsec rotating LGS.

3.1 NIR performance

The predicted AO performance in terms of an observed Strehl ratio in the *H* and *K* bands for rotating LGSs at 90 and 20 km is shown in Figs 9 and 10, respectively. It must be noted that this model assumes perfect detection and correction of the phase perturbations

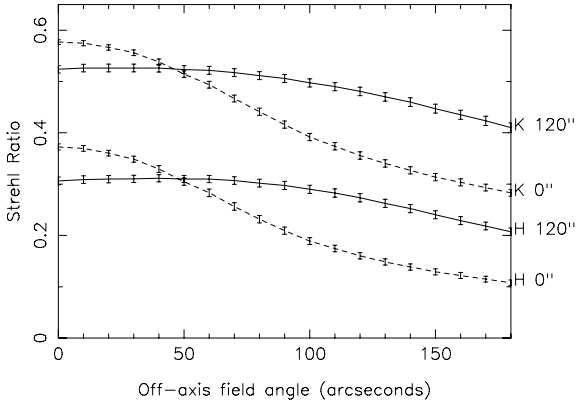

Figure 9. Performance of static (dashed line) and $\alpha = 120$ arcsec (solid line) rotating LGS created at an altitude of 90 km above an 8-m telescope aperture under the defined median atmospheric profile. *H*- and *K*-band plots were made under identical atmospheric r_0 and vertical turbulence distribution.

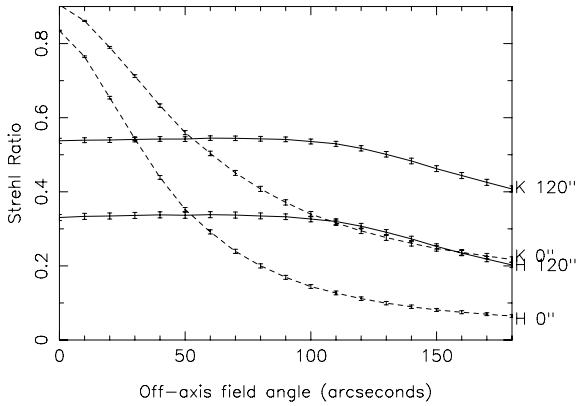

Figure 10. Performance of static (dashed line) and $\alpha = 120$ arcsec (solid line) rotating LGS created at an altitude of 90 km above an 8-m telescope aperture under the defined median atmospheric profile. *H*- and *K*-band plots were made under identical atmospheric r_0 and vertical turbulence distribution.

of the turbulent wavefront and therefore described the best-case scenario. Real-world AO systems will not meet the performances presented here under identical turbulence profiles as there are several error sources within any AO system that the model used here does not address. The Strehl ratio was calculated from the residual wavefront variance using the Maréchal approximation which is valid for residual phase variances of less than 1 rad^2, corresponding to a Strehl ratio of 0.37. In the case of the 90 km rotating LGS, irrespective of wavelength, a uniform Strehl ratio is returned across a field 200 arcsec in diameter, while a 20 km rotating LGS provides a uniform Strehl across a field 120 arcsec in diameter. The on-axis Strehl ratios of the rotating LGS at both LGS altitudes at each wavelength are similar, implying that the observed correction is not a function of the distance between the LGS and telescope pupil.

The on-axis Strehl ratio of a 20 km $\alpha = 120$ arcsec as shown in Fig. 10 is lower than that of an $\alpha = 60$ arcsec rotating LGS and static LGS. Fig. 11 demonstrates the potential Strehl ratio improvements when using an $\alpha = 60$ arcsec rotating LGS at a distance of 20 km compared to a static LGS. A marked improvement in Strehl ratio is observed at all field angles up to 180 arcsec off-axis in all wavelength bands.

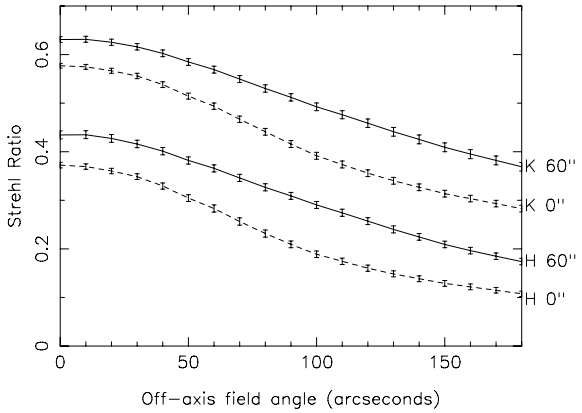

Figure 11. Performance of static (dashed line) and $\alpha = 60$ arcsec (solid line) rotating LGS created at an altitude of 20 km above an 8-m telescope aperture under the defined median atmospheric profile. *H*- and *K*-band plots were made under identical atmospheric r_0 and vertical turbulence distribution.

4 CONCLUSIONS

Several techniques for creating a rotating LGS and their performance have been presented. LGS rotation provides a signal that can give wide-field partial correction using a single LGS that is created at 8, 20 or 90 km vertical distance from the telescope aperture. The degree of wide-field correction is dependant upon the angular diameter of the LGS rotation. A larger angular rotation of the LGS will provide a larger field of uniform correction, albeit at the expense of the degree of that correction.

Importantly, the results also suggest that any AO system utilizing a single Rayleigh LGS should consider implementing a rotating LGS as this will improve not only the diameter of the uniformly corrected field but also the on-axis AO correction. Even for low-altitude Rayleigh LGS (below 10 km) that already exhibits GLAO-like performance, the effect of LGS rotation can both improve performance and increase the diameter of the uniformly corrected field of view. The modifications required to the launch and return optics of a static LGS to create a rotating LGS are minor, although on-sky implementation of this technique would undoubtedly uncover further technical issues.

The effect of altering the vertical distribution of turbulence within the first kilometre of atmosphere on the rotating LGS signal is small for an $\alpha = 60$ arcsec rotating LGS at a distance of 90 km. Increasing the strength of high-altitude turbulence degrades performance at both on-axis and off-axis field points, although there is very little change in the angular diameter of the corrected uniform field. This is in contrast to the performance of a static LGS where the angular diameter of the corrected field is affected by the vertical distribution of turbulence.

Future work on this concept will involve studying the decrease in WFS performance caused by the blurring of the WFS image, and, ultimately, this will be placed within the Durham Monte Carlo AO simulation (Basden et al. 2005) to study the performance of an AO system using a rotating LGS.

ACKNOWLEDGMENTS

The authors thank to Gordon Love and the referee for their useful comments made to improve this paper.

This work forms part of a technology development programme (ELT Design Study) supported by the European Community within its Framework Programme 6 under contract No. 011863.

REFERENCES

Basden A. G., Assémat T., Butterley T., Geng D., Saunter C. D., Wilson R. W., 2005, MNRAS, 364, 1413

Beckers J. M., 1989, in Roddier F. J., ed., SPIE Proc. Vol. 1114, Active Telescope Systems. SPIE, Bellingham, p. 215

Ellerbroek B. L. et al., 2003, in Wizinowich P. L., Bonaccini D., eds, SPIE Proc. 4839, Adaptive Optical System Technologies. SPIE, Bellingham, p. 55

Foy R., Labeyrie A., 1985, A&A, 152, L29

Gässler W. et al., 2004, in Calia D. B., Ellerbroek B., Ragazzoni R., eds, SPIE Proc. Vol. 5490, Advancements in Adaptive Optics. SPIE, Bellingham, p. 90

Hubin N. et al., 2002, in Vernet E., Ragazzoni R., Esposito S., Hubin N., eds, ESO Proc. Vol. 58, Beyond Conventional Adaptive Optics. ESO, Garching, p. 27

Kolb J. et al., 2004, in Calia D. B., Ellerbroek B., Ragazzoni R., SPIE Proc. Vol. 5490, Advancements in Adaptive Optics. SPIE, Bellingham, p. 794

Lloyd-Hart M., Baranec C., Mitton N. M., Stalcup T., Snyder M., Putnam N., Angel J. R. P., 2005, ApJ, 634, 679

Maréchal A., 1947, Rev. d'Optique, 26, 257
Noll R. J., 1976, J. Opt. Sci. Am., 66, 207
Ragazzoni R., 1999, in Andersen T., Ardeburg A., Gilmozzi R., eds, ESO Proc. Vol. 57, Backaskog Workshop on Extremely Large Telescopes. ESO, Garching, p. 175
Ragazzoni R., Farinato J., 1999, A&AS, 136, 205
Ragazzoni R., Marchetti E., Valente G., 2000, Nat, 403, 54
Riguat F., 2002, in Vernet E., Ragazzoni R., Esposito S., Hubin N., eds, ESO Proc. Vol. 58, Beyond Conventional Adaptive Optics. ESO, Garching, p. 11
Sharples R. M., Myers R. M., Walton N. A., 2000, in Masanori I., Moorwood A. F., eds, SPIE Proc. Vol. 4008, Optical and IR Instrumentation and Detectors. SPIE, Bellingham, p. 228
Tallon M., Foy R., 1990, A&A, 235, 549
Tokovinin A., 2004, PASP, 116, 941
Tokovinin A., Thomas S., Gregory B., van der Bliek N., Schurter P., Cantarutti R., Mondaca E., 2004, in Bonaccini D., Ellerbroek B., Ragazzoni R., eds, SPIE Proc. 5490, Advancements in Adaptive Optics. SPIE, Bellingham, p. 870
Tondusson M., Froehly C., Kermene V., Vampouille M., 2001, J. Opt. A:Pur. Ap. Opt., 3, 521
von Kármán T., 1948, Proc. Natl. Acad. Sci. USA, 34, 530
Wilson R. W., Jenkins C. R., 1996, MNRAS, 278, 39

This paper has been typeset from a TEX/LATEX file prepared by the author.